Structure, Vol. 9, 659–667, August, 2001, ©2001 Elsevier Science Ltd. All rights reserved. PII S0969-2126(01)00636-0

Structure-Based Development of Anticancer Drugs: Complexes of NAD(P)H:Quinone Oxidoreductase 1 with Chemotherapeutic Quinones

Margarita Faig,[1] Mario A. Bianchet,[1] Shannon Winski,[2] Robert Hargreaves,[3] Christopher J. Moody,[4] Anna R. Hudnott,[4] David Ross,[2] and L. Mario Amzel[1,5]

[1] Department of Biophysics and Biophysical Chemistry
Johns Hopkins Medical School
Baltimore, Maryland 21205

[2] School of Pharmacy and Cancer Center
University of Colorado Health Sciences Center
Denver, Colorado 80262

[3] CRC Drug Development Group
Patterson Institute for Cancer Research
Manchester, M20 4BX
United Kingdom

[4] School of Chemistry
University of Exeter
Exeter, Devon EX4 4QD
United Kingdom

Summary

Background: NAD(P)H:quinone acceptor oxidoreductase (QR1) protects animal cells from the deleterious and carcinogenic effects of quinones and other electrophiles. Remarkably, the same enzyme activates cancer prodrugs that become cytotoxic only after two-electron reduction. QR1's ability to bioactivate quinones and its elevated expression in many human solid tumors makes this protein an excellent target for enzyme-directed drug development. Until now, structural analysis of the mode of binding of chemotherapeutic compounds to QR1 was based on model building using the structures of complexes with simple substrates; no structure of complexes of QR1 with chemotherapeutic prodrugs had been reported.

Results: Here we report the high-resolution crystal structures of complexes of QR1 with three chemotherapeutic prodrugs: RH1, a water-soluble homolog of dimethylaziridinylbenzoquinone; EO9, an aziridinylindolequinone; and ARH019, another aziridinylindolequinone. The structures, determined to resolutions of 2.0 Å, 2.5 Å, and 1.86 Å, respectively, were refined to R values below 21% with excellent geometry.

Conclusions: The structures show that compounds can bind to QR1 in more than one orientation. Surprisingly, the two aziridinylindolequinones bind to the enzyme in different orientations. The results presented here reveal two new factors that must be taken into account in the design of prodrugs targeted for activation by QR1: the enzyme binding site is highly plastic and changes to accommodate binding of different substrates, and homologous drugs with different substituents may bind to QR1 in different orientations. These structural insights provide important clues for the optimization of chemotherapeutic compounds that utilize this reductive bioactivation pathway.

[5] Correspondence: mario@neruda.med.jhmi.edu

Introduction

NAD(P)H:Quinone acceptor oxidoreductase (EC 1.6.99.2; QR1 or NQO1; also called DT-diaphorase) is a flavoenzyme that catalyzes the obligatory two-electron reduction of quinones to hydroquinones [1]. This reaction prevents the one-electron reduction of quinones by cytochrome P450 reductase and other flavoproteins that would result in oxidative cycling with generation of deleterious radical species. In addition to its role in the detoxification of dietary quinones, the enzyme has been shown to catalyze the reductive activation of cancer chemotherapeutic quinones. Since QR1 is expressed at high levels throughout many human solid tumors such as thyroid, adrenal, breast, ovarian, colon, and non-small-cell lung cancer (NSCLC) [2], this enzyme has become an attractive target for enzyme-directed drug development.

Although the crystal structures of QR1 shed light on the enzyme mechanism [3, 4] and on the catalytic differences among species [4, 5], until now only molecular modeling has been used to obtain structural information about enzyme-prodrug interactions [6–8]. Most of these computer models have used information derived from our crystal structures of rat enzyme complexes with $NADP^+$ and the ternary complex with DQ [2,3,5,6-tetramethyl-1,4-benzoquinone] and CB (Cibacron® Blue 3GA), a strong QR1 inhibitor [3]. Unfortunately, these structures are not good models for the binding of simple substrates, because in both cases the ligands extend well beyond the substrate binding site. Recently, we reported the structures of the apo-hQR1 and the hQR1-DQ complexes [4], but these new structures have not yet been used in modeling studies. In any case, *direct* observation of the interaction of QR1 with chemotherapeutic prodrugs is necessary to understand sufficiently their mode of binding in order to assist in the optimization of this type of cytotoxic drug. In this paper, we report the crystal structures of complexes of recombinant human QR1 with a substituted aziridinylbenzoquinone and two aziridinylindolequinones, three drugs representing two families of compounds that have been used in clinical trials or are under preclinical development as potential QR1-directed antitumor agents.

Aziridinylbenzoquinones (AZQ; Figure 1) have undergone clinical trials as potential antitumor agents [9]. Both one- and two-electron reduction of these compounds produces activated aziridine groups that can crosslink DNA strands [10, 11]. The activated drugs react with the N7 position of guanine in DNA, with a sequence preference similar to that of other alkylating agents [12]. Among these drugs, MeDZQ [2,5-diaziridinyl-3,6-methyl-1,4-benzoquinone] (Figure 1 with X and X′ = methyl group)

Key words: DT-diaphorase; chemoprotection; cancer chemotherapy; reductive activation; indolequinones; diaziridinylbenzoquinone

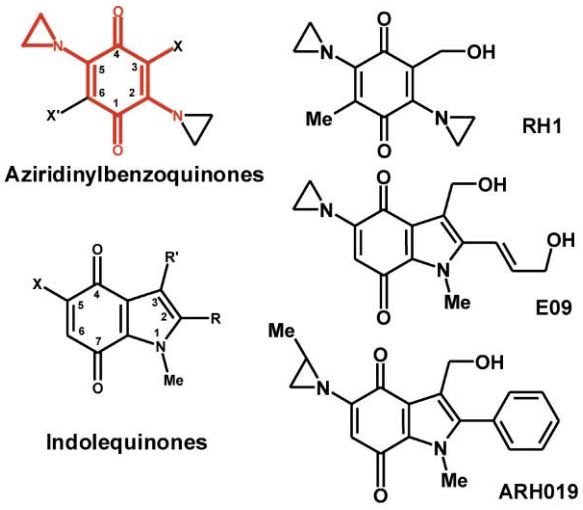

Figure 1. Drugs Used in the Present Study

Drug families are shown with R, R′, X, and X′ indicating the positions of substituents.

has been shown to be a good substrate for QR1, highly toxic in vitro for cell lines expressing high levels of the enzyme [13, 14]. MeDZQ also shows enhanced sequence specificity after reduction [11]. However, low solubility limits its use as a prodrug [11].

Using MeDZQ as a lead compound, several new drugs were synthesized in a second round of optimization that included changes in size and electronic characteristics of substituents at positions 3 and 6 [11, 15]. RH1 [2,5-diaziridinyl-3-hydroxyl-6-methyl-1,4-benzoquinone] (Figure 1), one of the compounds utilized in the present study, is an alkyl-substituted analog of MeDZQ that exhibits greater selective toxicity toward cells with elevated QR1 activity than does the parent compound [15]. We also report the crystal structures of two indolequinone drugs, EO9 [3-hydroxymethyl-5-aziridinyl-1-methyl-2-(H-indole-4,7-indione)-propenol] and ARH019 [3-hydroxymethyl-5-(2-methylaziridin-1-yl)-1-methyl-2-phenylindole-4,7-dione], in complex with QR1. These are members of a family of antitumor agents structurally related to the commonly used drug mitomycin C (MC). EO9 (Figure 1), the better known of these prodrugs, is reduced readily by rat QR1 (rQR1) but reduced 23 times slower by human QR1 (hQR1); it has a K_m 5-fold higher than menadione [16–18]. Nonetheless, EO9 is a better QR1 substrate than the clinically proven MC, and it shows high toxicity in QR1-rich cell lines [16]. Although partial responses in phase I trials were promising, subsequent phase II trials in cases that included NSCLC, breast, pancreatic, colorectal, and gastric tumors were disappointing. This failure has been attributed to poor delivery of EO9 to the tumor and to its rapid plasma clearance. These results motivated a search for drugs related to EO9 with better pharmacodynamic characteristics. One such compound, ARH019 (Figure 1), was developed [19] by keeping the important aziridinyl group at the indole position 5 where it is essential for potency and selectivity [20], but replacing the propenol group at the indole position 2 with a phenyl group. Here, we also report a high-resolution crystal structure of the hQR1 complex with ARH019.

The crystal structures reported here are used to compare the modes of binding of QR1 to the three chemotherapeutic drugs and to DQ, a simple acceptor substrate [4]. This analysis provides valuable information for the design of improved enzyme-directed chemotherapeutic agents.

Results and Discussion

Structure Determination and Refinement

The crystal structures of complexes of human QR1 enzyme with three potential chemotherapeutic compounds were determined and refined to R values lower than 21% with excellent stereochemistry (Table 1). Each structure has four copies of the hQR1-drug complex (four molecules in the asymmetric unit). Final $2F_o - F_c$ maps show excellent density for most portions of the polypeptide chains and for the four copies of the bound compounds (Figures 2a, 2b, and 2c). Ramachandran diagrams place over 87% of the residues in the most-favored regions.

All 12 copies of the QR1 structure refined in these crystals are highly similar, with some differences concentrated in the residues at one side of the active site over rings A and B of the flavin isoalloxazine. All four FAD molecules in each of the complexes show flat electron density for the isoallozaxine, indicating an oxidized state. Alignments of 546 α carbons of the apo human dimer (Protein Data Bank accession code 1D4A) with each the three complexes yield root-mean-square deviations (rmsd) in the range 0.26–0.34 Å (Table 1).

Overall Structure of the Enzyme and Active Site

QR1 is a physiological homodimer made of two interlocked monomers of 273 residues related by a noncrystallographic two-fold axis of symmetry. Each QR1 monomer is composed of two domains: a large catalytic domain (residues 1–220) and a small C-terminal domain (residues 221–273). (Residue numbers in this paper are those used in PDB, accession number 1D4A; they are shifted down by one residue with respect to those in some other publications.) The catalytic domain has an α/β fold with flavodoxin topology. All three prodrugs bind to the catalytic site of QR1 interacting with the bound FAD and with residues of both monomers. The catalytic site (Figure 3), a 360 $Å^3$ pocket, alternately binds the nicotinamide portion of the NAD(P)H and the electron acceptor substrate. This pocket is lined by residues from both monomers: Phe-178′, Tyr-126′, and Tyr-128′ form the roof of the active site; the isoalloxazine ring of FAD makes up the floor; and His-161, the N-terminal of L6′ (glycines 149 and 150), and two conserved water molecules (W1 and W2) flank the cavity. (When referring to the catalytic site, secondary structure elements and residues from individual monomers will be primed or unprimed. As the two monomers are equivalent, primes will be used only when distinction is needed.) In the active site, a structural water molecule and three groups of the protein—the hydroxyl groups of Tyr-126′ and Tyr-128′ and the Nϵ of His-161—are available to make hydro-

Table 1. Summary of the Crystallographic Analysis

Prodrug	RH1	EO9	ARH019
Resolution	2.0	2.5	1.86
Unique reflections	77,600	38,859	94,724
Multiplicity	3.9	3.7	3.5
Completeness (last shell)	95.0 (83.8) %	81.7 (81.3) %	93.7 (84.0) %
R_{sym}[a] × 100	9.1	8.4	7.3
Crystallographic Refinement			
Number of reflections used	73,718	35,866	74,185
Number of model atoms	9,676	9,092	9,295
Number of ligand atoms	280	296	308
Number of solvent atoms	707	104	295
R_{cryst}/R_{free}	19.9/25.6	19.9/27.9	20.9/25.7
Intensity cutoff	0.0	0.0	2.0
Rms bond/rms angles	0.008/1.3	0.008/1.39	0.008/1.37
Protein temperature factor (Å^2)	23.3	24.8	26.4
Ligands temperature factor (Å^2)	25.56	36.5	36.7
Solvent temperature factor (Å^2)	30.0	21.8	24.3
Surface buried apolar (Å^2)	447.0	492.0	584.5
polar (Å^2)	144.5	176.0	156.0
Occupancy factor	0.8	0.7	1.0
Drug temperature factor (Å^2)	38.5	26.0	56.0
Rms against Native dimer (number of Cα atoms)	0.22 (546)	0.23 (546)	0.20 (546)
PDB ID code	1H66	1GG5	1H69

[a] $R_{sym} = \Sigma_h\Sigma_j|I_{hj} - \langle I_h\rangle|/\Sigma_h\Sigma_j|I_{hj}|$, where h represents a unique reflection and j means symmetry equivalent indices. I is the observed intensity and $\langle I\rangle$ is the mean value of I.

gen bonds in the otherwise apolar pocket. As in the apo-QR1 structure, loop L9′ of the C-terminal domain closes the empty NAD adenosine site in all the complexes analyzed here.

Drug Binding

Introduction

Aziridinyl substituents have been shown to increase the potency and in vitro selectivity of quinolic drugs toward QR1-rich cells under aerobic conditions [7]. The three compounds examined in this study have in common a 1,4-benzoquinone core with an aziridinyl group at position 5. In addition, the 6-methyl carbon and the 2-aziridinyl nitrogen of RH1 occupy the positions of the indolequinone C3 and N1, respectively. For comparison, we define this set of 13 atoms as the common pharmacophore of the three drugs (shown in red in Figure 1).

The binding of the prodrugs to QR1 buries between 447 and 585 Å^2 of apolar accessible area of the protein (total buried area between 591 and 740 Å^2). All three drugs bind with their benzoquinone rings in one side of the pocket, stacked between Tyr-128′ and flavin rings A and B. Tyr-128′ swings over the substrate, making van der Waals contacts with the aromatic core of the drugs (Figures 2a, 2b, and 2c). RH1 and ARH019, a benzoquinone and an indolequinone, bind to QR1 with similar spatial arrangements such that their pharmacophore atoms overlap with a low rmsd of only 0.6 Å (Figure 4). Surprisingly, this is not the case with the two indolequinones EO9 and ARH019. Although chemically highly similar (they differ only in their substituents at positions 2 and 5), they bind to the enzyme in different orientations.

RH1 Binding

The two RH1 aziridinyl rings point away from the isoallozaxine ring, allowing the quinone core of the drug to interact fully with rings A and B of the flavin; the 5-aziridinyl group stacks against Trp-105, and that at position 2 (position numbering in Figure 1) rests above loop L6 (Figure 2a). His-194 has to move from its position in the apo structure to accommodate this last group. Quinone oxygens O1 and O4 make hydrogen bonds with the His-161 Nε and the Tyr-128′ OH (Table 2). The angle between the planes of the drug and the isoallozaxine is 15°, departing from the exact aromatic ring stacking observed in the rQR1 complexes with CB/DQ and $NADP^+$. The 5-aziridinyl nitrogen is the closest to the FAD N5, the atom of reduced FAD that carries the hydride that is transferred to the drug. Provided there is no change in the orientation of the bound substrate when the FAD is reduced, this atom will receive the hydride during the reduction of RH1.

ARH019 Binding

The ARH019 used was a mixture of both enantiomers of the methyl at position 2 of the aziridinyl group. The experimental electron density of the 2-methyl-aziridinyl shows a mixture of all four cases (two enantiomers and rotation around the aziridinyl-indole C5 bond), indicating that the enzyme does not select among these forms. As is the case in RH1, the plane of the ARH019 indolequinone departs from an exact aromatic parallel stacking with the FAD (plane-to-plane angle of 16°; Table 2). The methyl-aziridinyl group stacks against the Trp-105 indole. The 2-phenyl group points toward the outside of the active site pocket, stacking over Gly-149 and Gly-150 in L6 (Figure 2b). The structure of this complex illustrates how the enzyme's active site is capable of

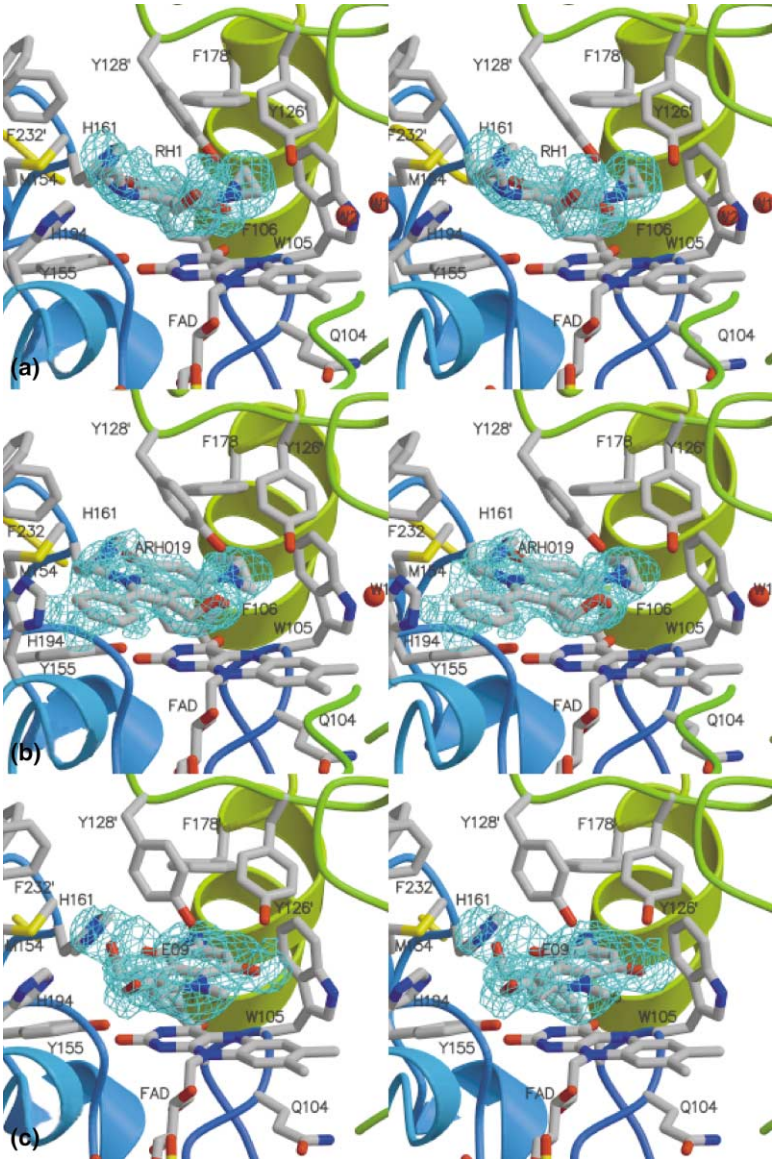

Figure 2. Stereo Views of Prodrug Molecules Bound to hQR1

In all the Figures the $2F_o - F_c$ electronic density around each drug is displayed in cyan. Secondary structure elements of monomers A (green) and B (light blue) are shown. QR1 residues, the FAD, and the drug are drawn using a stick model. Atoms are colored using the following scheme: red for oxygen, blue for nitrogen, gray for carbon, and yellow for phosphorous. (a) shows RH1, (b) shows ARH019, and (c) shows EO9.

accommodating a quinone with a large aromatic substituent. This compound can serve as a model for other drugs such as the antibiotic streptonigrin, another good substrate of the enzyme [16]. Quinone oxygens O7 and O4 are hydrogen bonded to the His-161 Nϵ and the Tyr-126′ OH. The 3-hydroxymethyl group further stabilizes the binding by making a hydrogen bond to Tyr-128′ OH.

EO9 Binding

Despite their chemical similarity, EO9 binds in an orientation opposite that of ARH019 (Figure 4); the positions of the pharmacophoric atoms do not match those described above. EO9 binding buries 176 Å^2 of polar area and 492 Å^2 of apolar area. Bound EO9 is more centered over the FAD isoallozaxine, is closer to ring B, and resembles DQ in the hQR1-DQ complex. The drug's plane is almost parallel to the isoallozaxine rings (angle of 3.6° ± 0.8°; Table 2) with its 5-aziridinyl group in the pocket defined by Phe-106. The distance from O7 to the His-161 Nϵ is 3.3 Å, indicating a weak hydrogen bond interaction. The other quinone oxygen atom, O4, is hydrogen bonded to Tyr-126′ OH. Indolequinone ring atom C6 is the closest to the FAD N5. The electron density observed for the 2-propenol tail is weak in some of the four equivalent sites, indicating that this group adopts multiple conformations in the binding site.

Relation between Drug Binding and Drug Reduction

Although the published information about the kinetics of the reduction of these three drugs is incomplete, it is clear that they are all better substrates for QR1 than the widely used MC. Human QR1 reduces RH1 (V_{max} 45.2 ± 2 μmol/min/mg) 6.5 times faster than EO9 (7.7 ± 2 μmol/min/mg) and 14 times faster than ARH019 (3.3 ± 2 μmol/min/mg) [7, 15, 16].

The reduction rates by QR1 of drugs similar to those described above show a strong correlation with the modes of binding suggested by the structures. Aziridinylbenzoquinones (Figure 1) tolerate large substitutions

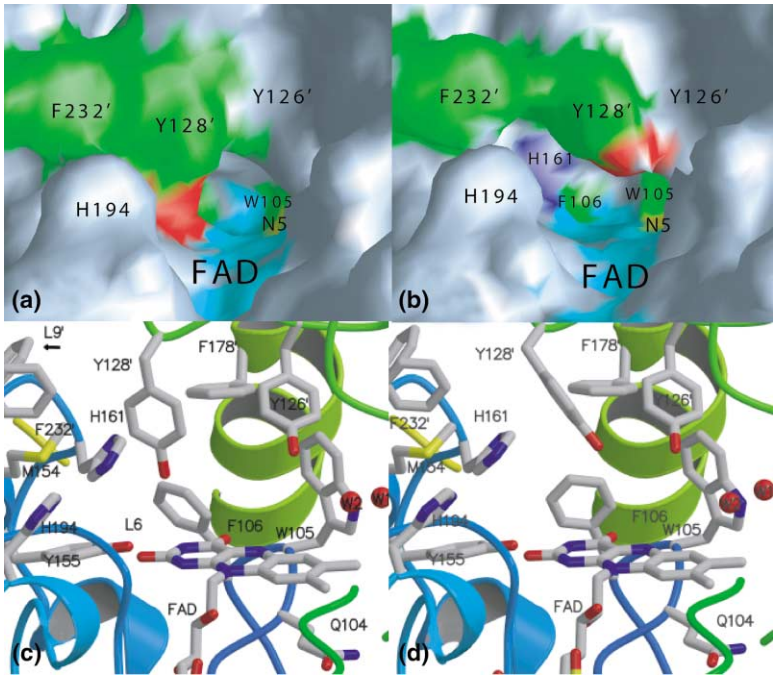

Figure 3. Changes in the Catalytic Site upon Drug Binding

(a) Water-accessible molecular surface of the apo enzyme. The surface of the pocket corresponding to F232′, Y128′, W105, and F106 is colored green (with the exception of the Y128′ OH, which is red), the FAD is cyan, and the small yellow patch indicates the position of the hydride (at the FAD's N5) to be transferred in the two-electron reduction of the drug.

(b) Water-accessible molecular surface of the drug bound form. In addition to the colors used in (a), H161 is colored purple.

(c) Stick model of the active site residues in the apo enzyme. The atoms are colored using the color scheme of Figure 2.

(d) Stick model of the drug bound active site. The atoms are colored using the color scheme of Figure 2.

only at position 3 (X) or at position 6 (X′). The RH1-QR1 complex shows that a substituent at one of these two positions points to the outside of the pocket, while the other position can only accommodate small substituents which point to the inside. Thus, drugs with progressively larger symmetrical substitutions have decreasing rates of reduction [13]. In the case of indolequinones (Figure 1), substituents (R) of different shapes and sizes are generally well tolerated at position 2 [7, 21]. The indolequinone-QR1 complexes show that substituents at this position point out of the binding pocket. A variety of small X substituents (position 5) are tolerated. At position 3, small size substituents (R′) have a small effect on the reduction rate, with electron-withdrawing groups increasing the rate. Compounds with three substituents of the type CH_2R (R = leaving group) inactivate the enzyme [19].

EO9 and ARH019 bind hQR1 in dissimilar ways, although both are aziridinylindolequinones. The kinetics of reduction of a group of closely related compounds (EO9 homologs studied by Bailey et al. [22] and ARH019 homologs studied by Beall et al. [19]) illustrate the effect of small differences in the substituents (X) at position 5 (Figure 5). If one assigns to these compounds a putative binding mode based on their homology with EO9 or ARH019 (Figure 5), analysis of the published data suggests a correlation between the binding orientation and the rate of reduction by the enzyme. The normalized reduction activities (Figure 5) of the members of set A (predicted to bind like EO9) and set B (predicted to bind like ARH019) display a similar effect with the change of the substituent at position 5 (X-substituent). EO9 (compound A2) has the highest reduction rate of the EO9-like compounds; compounds with slightly longer substituents such as E07 (A1) and EO8 (A3) are reduced at lower rates [7, 22]. Compound EO5A (A4), which has the bulkiest X substituent, is not reduced by QR1. In contrast, compound B4 is a QR1 substrate, although with a 10-fold reduction in rate. This indicates that the enzyme can accommodate bulky 5-substituents more efficiently in compounds that bind like ARH019 (orientation B) than in compounds that bind like EO9 (orientation

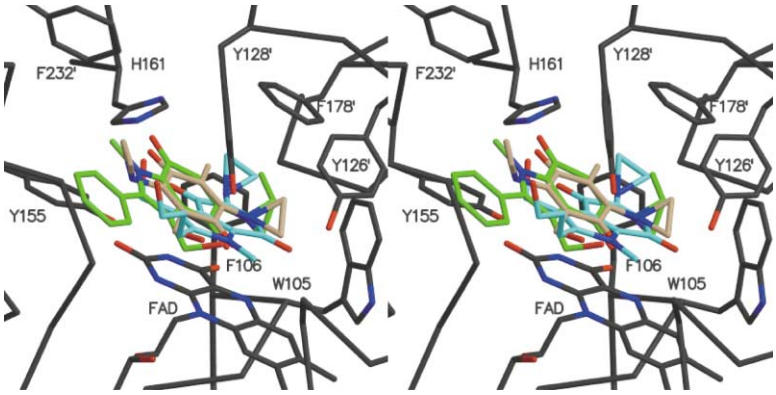

Figure 4. Stereo View of the Superposition of the Three Drugs in the Catalytic Site

The drugs' carbon atoms are colored pink for RH1, green for ARH019, and light blue for E09. The model of the protein of the complex (RH1-hQR1) was used to represent the binding site.

Table 2. Interactions between the Prodrugs and hQR1

Enzyme/FAD Atom	RH1	Distance (Å)	E09	Distance (Å)	ARH019	Distance (Å)
His 161 Nϵ	O1	2.9 ± 0.2	O4	3.3 ± 0.2	O7	3.0 ± 0.1
FAD N5	N5	3.5 ± 0.3	C6	3.6 ± 0.1	N5	3.8 ± 0.2
	C51	3.4 ± 0.2	C5	3.8 ± 0.05	C51	3.5 ± 0.2
	C5	4.4 ± 0.3	O7	3.8 ± 0.1		
	C4	4.8 ± 0.3				
	O4	4.6 ± 0.2				
FAD N10	O4	3.5 ± 0.3	N1	3.5 ± 0.1	O4	3.3 ± 0.1
Tyr-126′ OH			O7	2.9 ± 0.1		
Tyr-128′ OH	O4	3.3 ± 0.2	N1	3.3 ± 0.2	O31	2.5 ± 0.3
Angle between planes (FAD/prodrug)		15.0 ± 5°		3.6 ± 0.8°		16.0 ± 3.1°
Angle between planes (178/prodrug)		8.5 ± 4.5°		13.5 ± 2.7°		27.7 ± 5.7°

A). In addition to these effects, the electronic characteristics of the substituents also affect the reduction rates, mainly by affecting the reduction potential of the compounds [19].

Sequence identities among the three species for which QR1 structural data is available are 86% for rat and human, 93% for mouse and rat, and 86% for human and mouse. Most natural substrates (e.g., menadione) are reduced two to four times faster by the rat than by the human enzyme [5, 23]. The K_ms of rQR1 for EO9 and MeDZQ (RH1's parent drug) are 2-fold lower than those of the human enzyme, with a V_{max} range 2–3 times larger [16]. mQR1, whose structure [4] and kinetic profile resemble those of hQR1 [5], has been shown to have K_ms for RH1 and EO9 in the order of 10^{-5} M. Only a few differences between the enzymes from rats and humans have a direct effect on the catalytic site and can provide a rationale for the differences in catalytic efficiency. For example, the Thr/Ala-130 and Tyr/Gln-104 (rat/human) differences result in the largest change in the structure of the active site [4]: a tilt of the FAD isoallozaxine ring such that ring C in the human enzyme sits 0.5 Å deeper in the active site than it does in the rat enzyme [4]. As kinetic data are not available for RH1 and ARH019 reduction by rQR1, it is only possible to extrapolate from the data of the RH1 parent compound MeDZQ, which shows the typical 4-fold increase in rate from hQR1 to rQR1. Interestingly, species differences have a greater effect on EO9, which is reduced 27 times faster by rQR1 than by hQR1. The binding position of EO9, which is closer to the center of the active site than the other compounds are, apparently makes the drug more susceptible to the change in the FAD position.

Mouse QR1 (mQR1), although more similar in overall sequence to rQR1 than to hQR1, contains the key residues Ala-130 and Gln-104 found in the human sequence. In agreement with the discussion above, the kinetics of hQR1 reactions is more similar to that of mQR1 than to that of rQR1. Thus, mouse would be a better experimental system for testing QR1-activated prodrugs than rat, which is the animal model currently used.

Mechanism of Drug Reduction

As was observed in hQR1-DQ and rQR1/CB-DQ, the quinone ring carbon atoms seem to be in the best positions to accept the hydride from $FADH_2$ (Table 2). In all three complexes reported here, one of the quinone oxygens interacts closely with the His-161 Nϵ (distance 3.0–3.3 Å). Since the quinone oxygen can only participate in a hydrogen bond as a proton acceptor, the His-

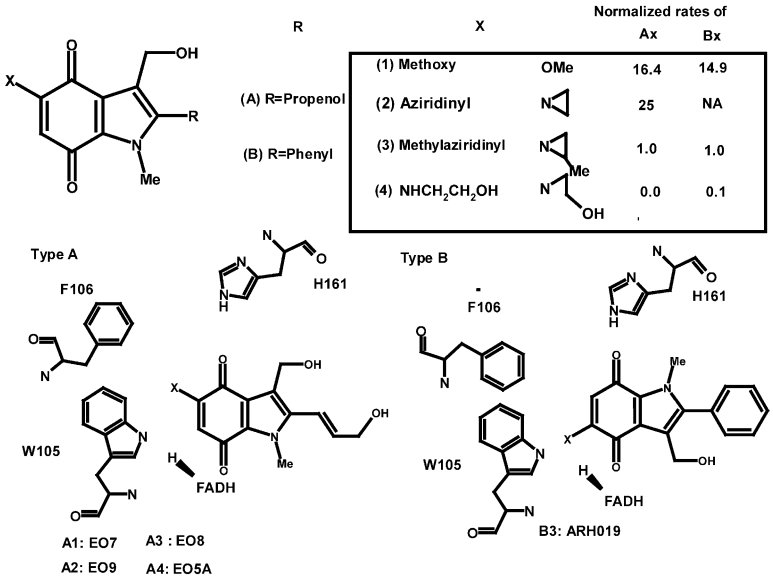

Figure 5. Reduction of Antitumor Prodrugs

Top panel: Nomenclature and the dependence of the reduction rate with small variations in size of the X substituent in indolequinones related to E09 and ARH019. The reduction rates are normalized to the rate of the methylaziridinyl (3) substituted compound of each subfamily.

Bottom panel: Scheme of the two putative modes of binding for each subfamily.

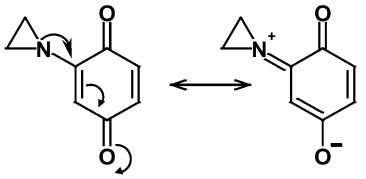

Figure 6. Resonance of the Aziridinyl Benzoquinone

This resonance is suggested as the form that accepts the hydride from the $FADH_2$. The negative charge at the quinolic oxygen is stabilized by a hydrogen bond to the positively charged H161.

161 imidazole must be protonated at Nϵ when the quinones are bound to QR1. In the proposed mechanism [3], $FADH_2$ is in the enolic form. O2F captures the proton from Tyr-155, thereby generating a negative charge (tyrosinate anion) for which the nearby His-161 compensates either by a proton transfer or simply by becoming positively charged. Of these two possibilities, charge compensation is the most likely, because a direct proton transfer from the imidazole to Tyr-155 would have to take place across a long distance (4.0 Å) and with an unfavorable angle. Therefore, release of $NAD(P)^+$ from the reduced enzyme must be accompanied by protonation of the Nδ of His-161 to produce a positively charged imidazole. Analysis of the hydrogen bonding pattern of QR1 structures indicates that the Nδ of His-161 is hydrogen bonded to the OH of Tyr-132′ (2.8 Å), which in turn binds to a well-conserved chain of hydrogen bonded atoms, many of them structural water molecules. This proton wire connects to the bulk solvent and can easily shuttle protons in and out to change the protonation state of His-161 during catalysis.

During reduction of the substrate, the hydride is transferred from the $FADH_2$ to the quinone, and the charge reorganizes. Tyr-155 reprotonates and the Nϵ proton of His-161 is transferred to the reduced quinone. After release of the reduced quinone, solvent molecules can permeate the catalytic site and protonate the His-161 Nϵ, while Nδ loses its proton via Tyr-132. This step is driven by the higher basicity of Nϵ (pKa difference is 0.6 units for free histidine). In summary, all these complexes seem to indicate that His-161 has two roles in the catalytic cycle: it compensates the charge in Tyr-155 after flavin reduction and $NAD(P)^+$ release, and it provides a proton to the quinone oxygen during hydride transfer, i.e., it is the proton donor required for the overall reaction $FADH_2$ + quinone + $H^+ \leftrightarrow FAD^+$ + hydroquinone.

One remaining question is the nature of the atom that receives the hydride from the reduced flavin. In the cases of RH1 and ARH019, the nitrogen of the aziridinyl group is best *located* for accepting the hydride (Table 2). In general, the aziridinyl nitrogen would not be a good hydride acceptor. However, in the case of aziridinyl quinones, the resonance shown in Figure 6 can render this atom a better hydride acceptor. His-161 is ideally located to stabilize this resonance form by donating a proton to the negatively charged oxygen. The existence of this resonance form is supported by the experimental electron density that shows that the nitrogen of the aziridinyl group is more planar that what can be expected for an sp^3 hybridization.

Catalytic Site Changes upon Drug Binding

The structural changes associated with substrate binding occur at one side of the binding pocket (Figure 3) and involve only a few residues located above isoallozaxine rings A and B. Phe-106, Tyr-128′, and Phe-232′ show the largest displacements with respect to the apo-hQR1 structures reported earlier [4].

In the case of the binding of DQ, RH1, and ARH019, the movement of the Phe-106 side chain controls the accessibility to the pocket defined by Phe-106 itself, Trp-105, Phe-178′, and the main chain of Ile-175′. Phe-106 rotates from its position in apo-hQR1 so as to increase the pocket complementarity to the substrates. When EO9 binds to hQR1, the pocket opens to make room for the group at position 5. The side chain of Tyr-128 has the largest freedom of movement in the active site, being constrained only by Phe-232. In rQR1/CB-DQ and $rQR1/NADP^+$, Tyr-128 occupies similar positions and interacts either with the nicotinamide (in the $rQR1\text{-}NADP^+$ complex), or with the CB triazine ring and DQ (in the rQR1/CB-DQ) [3]. In the structures of apo-mQR1 and apo-hQR1, this tyrosine swings back into the catalytic site and, together with Phe-232, closes the NAD(P) binding site [4]. This seems to be the preferred conformation when there are no molecules occupying the region just over ring A, and this conformation protects this side of the binding site from the solvent. In the hQR1-DQ complex, Tyr-128 binds DQ through a water molecule. Nevertheless, in all three complexes reported in this paper, Tyr-128 is present in a conformer that more closely resembles that observed in the ternary complex rQR1/CB-DQ than that in apo-(h/m)QR1 or hQR1-DQ.

Other residues also contribute to the binding of these drugs. Trp-105 and Phe-106 participate by forming a hydrophobic pocket where one of the substrate's 5-aziridinyl groups docks. Residues Gly-149, Gly-150 (in L6), and His-194 form a pocket in one side of the mouth of the catalytic site. They provide van der Waals contacts with substituents at position 2 of the quinone ring such as the aziridinyl of RH1, the phenyl of ARH019, and (partially) the propenol chain of EO9.

Biological Implications

QR1 is an inducible cytosolic enzyme that protects the organism against the deleterious effects of quinones and other electrophiles. Paradoxically, the same two-electron reaction that inactivates quinones can activate certain chemotherapeutic prodrugs, thereby rendering them cytotoxic. Two additional properties of QR1 make this enzyme an ideal target for the development of antitumor compounds activatable by two-electron reductions. First, QR1 is inducible in normal tissues. Second, the enzyme is constitutively expressed in some important tumors such as non-small-cell lung, breast, pancreatic, colorectal, and gastric cancers. A large number of QR1-directed compounds have been synthesized and tested, but no structural information on their interaction with QR1 has been available. The three structures of complexes of QR1 with chemotherapeutic prodrugs reported here provide evidence for two important charac-

teristics of QR1-drug binding: first, QR1 modifies the shape of its binding site to accommodate different compounds, and second, compounds of similar structure may bind to QR1 in different orientations. The ability to accommodate different compounds is accomplished primarily by movements of the side chains of two residues: Tyr-128′ of one monomer moves to accommodate the main ring of the drugs, and Phe-106 of the other monomer moves to accommodate the 5-aziridinyl group. The structures also suggest that because of its interaction with the pocket defined by loop L6, the substituent at position 2 plays an important role in drug binding, particularly in its size, flexibility, and hydrophobic character. As a result of these requirements, compounds as homologous as EO9 and ARH019 bind to the enzyme in dissimilar orientations, while the chemically different RH1 and ARH019 bind to QR1 in similar orientations. Significantly, the in vitro kinetic behavior of these and related compounds shows a strong correlation with the mode of binding revealed by the structures.

The structures also highlight the importance of His-161 in the mechanism of the enzyme. This residue is the catalytic acid necessary to protonate the reduced quinone. Initially, it acts as a hydrogen bond donor for binding the quinone substrate. Following hydride transfer, the same proton is transferred to the reduced quinone to produce a neutral species that leads to product formation.

Experimental Procedures

Materials

The expression of human recombinant QR1 in *E. coli* and its subsequent purification were carried out using methods described previously [24]. The synthesis of RH1 is described by Hargreaves et al. [25], and the synthesis of ARH019 is described by Moody and coworkers [19].

Crystallization and Data Collection

HQR1 crystals, grown as described before [4], belong to the triclinic space group P1 with cell dimensions $a = 55.7$ Å, $b = 57.0$ Å, $c = 97.4$ Å, $\alpha = 76.7°$, $\beta = 77.0°$, and $\gamma = 86.0°$. The crystals contain two physiological dimers in the asymmetric unit. The complexes were obtained by soaking the native crystals overnight in mother liquor solutions containing the prodrugs in the following concentrations: 200 μM of RH1, 10.0 mM of EO9, and 3.0 mM of ARH019. A stock solution (5–10 mg/ml) in DMSO was used to prepare complexes 1 and 2; acetonitrile was used as a solvent to prepare complex 3.

All diffraction data were collected at the National Synchrotron Light Source of the Brookhaven National Laboratory at beam line X25, using a wavelength of 1.1 Å and a Brandeis charge-coupled device (CCD) detector. Data for the hQR1 complexes were collected at 100 K after flash freezing by immersion in liquid nitrogen in unmodified mother liquor. The data were reduced with the software package HKL [26].

Structure Determination and Refinement

Initial structures were modeled by the use of the coordinates of the apo-hQR1 structure (PDB accession code 1D4A). For each of the complexes, the positions of the four monomers were refined independently as rigid bodies. Difference-Fourier electron density maps calculated after convergence showed density for the compounds in the four active sites. Drug models were built with parameters and topologies derived from related compounds, including *p*-benzoquinones reported in the Cambridge Structural Database [27]. The structural models of the complexes were refined with the program CNS [28]. We tested for the possibility of alternative orientations of the drugs in the active site in all the compounds. The final conformations we are reporting are the only ones that produce featureless $F_o - F_c$ difference maps after refinement. All other orientations resulted in difference maps with significant positive and negative features that suggested changes leading to the reported orientations. In addition, the reported orientations showed the best chemical interactions with active site residues. A torsional molecular dynamics refinement, either at constant temperature (2000 K) or as a slow-cooling annealing, was followed by energy minimization, restrained B factor refinement, and manual rebuilding in SIGMAA-weighted maps with the program O [29]. Figures were drawn with the programs MOLSCRIPT [30], BOBSCRIPT [31], and RASTER3D [32]. Structure quality was assessed with the program PROCHECK, which is part of the CCP4 suite of programs [33]. Molecular surfaces were drawn with the program GRASP [34]. Solvent accessible surface areas (ASA) were calculated with the program NACCESS [35].

Acknowledgments

Our research was supported by grant GM45540 from the National Institute of General Medical Sciences to L.M.A. and grant CA51210 from the National Cancer Institute to D.R. We thank Drs. Lonny Berman, Hal Lewis (X25), and Craig Ogata (X4A) for help and guidance at the synchrotron beam lines.

Received: February 28, 2001
Revised: June 28, 2001
Accepted: July 9, 2001

References

1. Ernster, L., and Navazio, F. (1958). Soluble diaphorase in animal tissues. Acta Chem. Scand. *12*, 595–602.
2. Siegel, D., and Ross, D. (2000). Immunodetection of NAD(P)H:quinone oxidoreductase 1 (NQO1) in human tissues. Free Radic. Biol. Med. *29*, 246–253.
3. Li, R., Bianchet, M., Talalay, P., and Amzel, L. (1995). The three-dimensional structure of NAD(P)H:quinone reductase, a flavoprotein involved in cancer chemoprotection and chemotherapy: mechanism of the two-electron reduction. Proc. Natl. Acad. Sci. USA *92*, 8846–8850.
4. Faig, M., et al., and Amzel, L.M. (2000). Structures of recombinant mouse and human NAD(P)H:Quinone Oxidoreductases: Species comparison and structural changes with substrate binding and release. Proc. Nat. Acad. Sci. USA *97*, 3177–3182.
5. Chen, S., et al., and Amzel, L. (1997). Molecular basis of the catalytic differences among DT-diaphorase of human, rat, and mouse. J. Biol. Chem. *272*, 1437–1439.
6. Chen, S., Wu, K., Zhang, D., Sherman, M., Knox, R., and Yang, C. (1999). Molecular characterization of binding of substrates and inhibitors to DT-diaphorase: combined approach involving site-directed mutagenesis, inhibitor-binding analysis, and computer modeling. Mol. Pharmacol. *56*, 272–278.
7. Phillips, R.M., et al., and Stratford, I.J. (1999). Bioreductive activation of a series of indolequinones by human DT-diaphorase: structure-activity relationships. J. Med. Chem. *42*, 4071–4080.
8. Skelly, J., et al., and Neidle, S. (1999). Crystal structure of human DT-diaphorase: a model for interaction with the cytotoxic prodrug 5-(aziridin-1-yl)-2,4-dinitrobenzamide (CB1954). J. Med. Chem. *42*, 4325–4330.
9. Schold, S.C., Jr., Friedman, H.S., Bjornsson, T.D., and Falletta, J.M. (1984). Treatment of patients with recurrent primary brain tumors with AZQ. Neurology *34*, 615–619.
10. Lee, C., et al., and Gibson, N. (1992). Alteration in DNA cross-linking and sequence selectivity of a series of aziridinylbenzoquinones after enzymatic reduction by DT-diaphorase. Biochemistry *31*, 3019–3025.
11. Hargreaves, R., O'Hare, C.C., Hartley, J., Ross, D., and Butler, J. (1999). Cross-linking and sequence-specific alkylation of DNA by aziridinylquinones. 3. Effects of alkyl substituents. J. Med. Chem. *42*, 2245–2250.
12. Siegel, D., Gibson, N., Preusch, P., and Ross, D. (1990). Metabolism of diaziquone by NAD(P)H:(quinone acceptor) oxidoreductase (DT-diaphorase): role in diaziquone-induced DNA damage

and cytotoxicity in human colon carcinoma cells. Cancer Res. *50*, 7293–7300.
13. Gibson, N., Hartley, J., Butler, J., Siegel, D., and Ross, D. (1992). Relationship between DT-diaphorase-mediated metabolism of a series of aziridinylbenzoquinones and DNA damage and cytotoxicity. Mol. Pharmacol. *42*, 531–536.
14. Ross, D., Beall, H., Traver, R.D., Siegel, D., Phillips, R.M., and Gibson, N.W. (1994). Bioactivation of quinones by DT-diaphorase, molecular, biochemical, and chemical studies. Oncol. Res. *6*, 493–500.
15. Winski, S., Hargreaves, R., Butler, J., and Ross, D. (1998). A new screening system for NAD(P)H:quinone oxidoreductase (NQO1)-directed antitumor quinones: identification of a new aziridinylbenzoquinone, RH1, as a NQO1-directed antitumor agent. Clin. Cancer Res. *4*, 3083–3088.
16. Beall, H., Murphy, A., Siegel, D., Hargreaves, R., Butler, J., and Ross, D. (1995). Nicotinamide adenine dinucleotide (phosphate): quinone oxidoreductase (DT-diaphorase) as a target for bioreductive antitumor quinones: quinone cytotoxicity and selectivity in human lung and breast cancer cell lines. Mol. Pharmacol.*48*, 499–504.
17. Walton, M., Smith, P., and Workman, P. (1991). The role of NAD(P)H: quinone reductase (EC 1.6.99.2, DT-diaphorase) in the reductive bioactivation of the novel indoloquinone antitumor agent EO9. Cancer Commun. *3*, 199–206.
18. Maliepaard, M., Wolfs, A., Groot, S.E., de Mol, N.J., and Janssen, L. (1995). Indoloquinone EO9: DNA interstrand cross-linking upon reduction by DT-diaphorase or xanthine oxidase. Br. J. Cancer *71*, 836–839.
19. Beall, H.D., et al., and Moody, C.J. (1998). Indolequinone antitumor agents: correlation between quinone structure, rate of metabolism by recombinant human NAD(P)H:quinone oxidoreductase, and in vitro cytotoxicity. J. Med. Chem. *41*, 4755–4766.
20. Phillips, R. (1999). Inhibition of DT-diaphorase (NAD(P)H:quinone oxidoreductase, EC 1.6.99.2) by 5,6-dimethylxanthenone-4-acetic acid (DMXAA) and flavone-8-acetic acid (FAA): implications for bioreductive drug development. Biochem. Pharmacol. *58*, 303–310.
21. Moody, C.J., and Swann, E. (1997). Novel bioreductive anticancer agents based on indolequinones. Farmaco *52*, 271–279.
22. Bailey, S., Suggett, N., Walton, M., and Workman, P. (1992). Structure-activity relationships for DT-diaphorase reduction of hypoxic cell directed agents: indoloquinones and diaziridinyl benzoquinones. Int. J. Radiat. Oncol. Biol. Phys. *22*, 649–653.
23. Chen, S., et al., and Tsai, T. (1995). Catalytic properties of NAD(P)H:quinone acceptor oxidoreductase: study involving mouse, rat, human, and mouse-rat chimeric enzymes. Mol. Pharmacol. *47*, 934–939.
24. Chen, H., Ma, J., Forrest, G., Deng, P., Martino, P., Lee, T., and Chen, S. (1992). Expression of rat liver NAD(P)H:quinone-acceptor oxidoreductase in Escherichia coli and mutagenesis in vitro at Arg-177. Biochem. J. *284* (Pt 3), 855–860.
25. Winski, S.L., Hargreaves, R.H., Butler, J., and Ross, D. (1998). A new screening system for NAD(P)H:quinone oxidoreductase (NQO1)-directed antitumor quinones: identification of a new aziridinylbenzoquinone, RH1, as a NQO1-directed antitumor agent. Clin. Cancer Res. *4*, 3083–3088.
26. Otwinowski, Z.M., W. (1997). Processing of X-ray diffraction data collected in oscillation mode. Methods Enzymol. *277*, 307–326.
27. Allen, F.H., and Kennard, O. (1993). 3D search and research using the cambridge structural database. Chem. Des. Automation News *8*, 31–37.
28. Brunger, A., Adams, P., Clore, G., DeLano, W., Gros, P., Grosse-Kunstleve, R., Jiang, J., Kuszewski, J., Nilges, M., Pannu, N., Read, R., Rice, L., Simonson, T., and Warren, G. (1998). Crystallography & NMR system: A new software suite for macromolecular structure determination. Acta Crystallogr. D *54*, 905–921.
29. Jones, T.A., Zou, J.Y., Cowan, S.W., and Kjeldgaard, M. (1991). Improved methods for building protein models in electron density maps and the location of errors in these models. Acta Crystallogr. A *47*, 110–119.
30. Kraulis, P. (1991). Molscript. J. Appl. Crystallogr. *24*, 946–950.
31. Esnouf, R.M. (1997). An extensively modified version of MolScript that includes greatly enhanced coloring capabilities. J. Mol. Graph. Model. *15*, 132–134.
32. Merrit, E.A., and Bacon, D.J. (1997). RASTER3D. Methods Enzymol. *277*, 505–524.
33. CCP4 (Collaborative Computational Project 4) (1994). The CCP4 suite: programs for protein crystallography. Acta Crystallogr. D *50*, 760–763.
34. Nicholls, A., Sharp, K.A., and Honig, B. (1991). Protein folding and association: insights from the interfacial and thermodynamic properties of hydrocarbons. Proteins *11*, 281–296.
35. Hubbard, S., and Thornton, J. (1993). 'NACCESS' Computer Program, Department of Biochemistry and Molecular Biology (London: University College).

Accession Numbers

The atomic coordinates have been deposited in the Protein Data Bank with the following numbers: 1H66 for the hQR1-RH1 complex, 1GG5 for the hQR1-EO9 complex, and 1H69 for the hQR1-ARH019 complex.